

Magnetic Study of the Novel Polynuclear Compound [Cu(II)(6-Mercaptopurinolate²⁻)]_n

Rodolfo Acevedo-Chávez

Centro de Química, Instituto de Ciencias, B. Universidad Autónoma de Puebla, Apartado Postal 1613, Puebla, Puebla, México

María Eugenia Costas¹

Facultad de Química, Universidad Nacional Autónoma de México, México 04510, D.F., México

and

Roberto Escudero

Instituto de Investigaciones en Materiales, Universidad Nacional Autónoma de México, México 04510, D.F., México

Received July 29, 1996; in revised form April 1, 1997; accepted April 3, 1997

Chemical reactions between Cu(II) and 6-mercaptopurine, both in aqueous and in methanolic media, yield the novel amorphous polynuclear compound [Cu(II)(6-mercaptopurinolate²⁻)]_n, which is also obtained from diverse Cu(II)–heterocyclic ligand competitive reactions. The kinetic and thermodynamic stabilities associated with the formation of this compound are inferred as remarkable. The spectroscopic data let us suggest the involvement of the exocyclic S(6) donor site and the N atoms in the imidazolic moiety of the deprotonated heterocyclic ligand in the coordination to Cu(II) atoms, forming a distorted bidimensional metallic network. The magnetic studies show the existence of very weak antiferromagnetic coupling in the solid sample. This system represents the first example of a 1:1 metal:6-mercaptopurinolate²⁻ system with a *d*-type open shell metallic center. The magnetic study carried out also represents the first example of magnetic characterization for this type of polynuclear Cu(II) systems with the dianionic 6-mercaptopurine ligand. © 1997

Academic Press

INTRODUCTION

Purine derivatives are interesting molecules due to their very rich acid–base physical chemistry, to the variety of metallic bonding sites they show in the correspondent coordination compounds, and to their stereochemical, spectral, and physical properties, among other features.

The synthetic (1,2) heterocycle 6-mercaptopurine (Fig. 1) is the structural analogue of the ribonucleic acid minor base

6-oxopurine (hypoxanthine); it is employed against certain neoplastic diseases, as acute lymphoblastic leukemia (3).

This fact, together with the specific role that several transitional metals play in the nucleic acid processes (4), has prompted several research groups to carry out studies related to the metallic bonding behavior of 6-mercaptopurine (and its nucleosides, nucleotides, and derivatives) in coordination compounds (5). From these studies it is important to arise the key role played by the exocyclic S(6) atom in the metallic bonding of the molecule: as terminal or bridge ligand through the S(6) atom, as chelating ligand through the S(6) and N(7) atoms, or even more and interestingly, as chelating ligand toward a metallic center (S(6) and N(7)) and simultaneously bridging (through S(6)) adjacent metallic centers in scarce polynuclear coordination compounds (6). To our knowledge, there is no report of a compound where this exocyclic S atom reluctes to bond to transition metallic centers. This behavior may be associated with the great electronic exchange capability and the energetic and spatial disposition of the orbitals of this atom.

In our research program related to the study of transition metallic center–purine derivative interactions, we have explored the reactions of 6-mercaptopurine with Cu(II) under several experimental conditions, and we have confirmed the great reactivity and bonding capability of the heterocyclic ligand through the S(6) atom.

In this paper we report several Cu(II)–6-mercaptopurine reactions carried out both in aqueous (at different pH values) and in methanolic media, including competitive reactions of this heterocycle with other ligands (for example,

¹ To whom correspondence should be addressed.

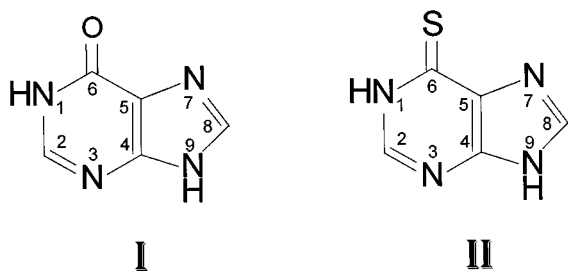


FIG. 1. Schematic drawing and numbering of 6-oxopurine (I) and its structural analogue 6-mercaptapurine (II).

6-oxopurine or its isomer, allopurinol) toward the Cu(II) coordination sphere. Also, we report here the spectral and magnetic study of the novel polynuclear coordination compound $[\text{Cu(II)(6-mp}^{2-})]_n$ (6-mp $^{2-}$, 6-mercaptapurinate $^{2-}$), which is the unique product in these metal–ligand reactions.

EXPERIMENTAL

Reagents

The Cu(II) metallic salts ($X = \text{Cl}^-$, Br^- , NO_3^- , SO_4^{2-} , ClO_4^- , and CH_3CO_2^-), 6-mercaptapurine, 6-oxopurine, allopurinol, buffers (glycine/HCl/NaCl for pH 1; $\text{CH}_3\text{CO}_2\text{H}/\text{NaCH}_3\text{CO}_2$ for pH 4; $\text{KH}_2\text{PO}_4/\text{K}_2\text{HPO}_4$ for pH 7; and KOH/KCl for pH 13), and organic solvents were commercially acquired. All were used with no further purification.

Cu(II)–Heterocycle Reactions

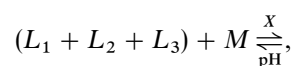
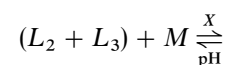
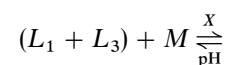
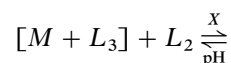
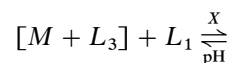
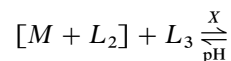
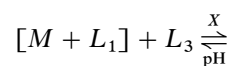
Aqueous Medium

All the reactions were independently carried out at pH values of 1, 4, 7, and 13. Also, for each one of them, the metallic counterion (from Cl^- to CH_3CO_2^-) was systematically changed.

Cu(II)–6-mercaptapurine reactions. At each pH value, 1 mmol of 6-mercaptapurine was added to 100 ml of the buffer solution, and the mixture was allowed to boil under stirring and refluxing at atmospheric pressure. One millimole of the respective metallic salt (previously dissolved in ca. 10 ml of H_2O) was added to the resulting pale yellow solution, shortly forming a green suspension, which was maintained under those conditions for several days; no changes were observed. The boiling mixture was filtered off, and the solid product (dark green) was purified by washing it exhaustively, first with boiling H_2O and then with boiling CH_3OH . The product obtained from each reaction was kept at ca. 100°C for 24 hours. Under these conditions, the solid showed a noticeable dark green color, due to the density increase of the sample. The original color was again ob-

tained when each sample was finely powdered. This same product was obtained when 1:2 and 1:3 metal:ligand molar ratios were used for each metallic salt and pH value. The compound synthesized in all these reactions was almost insoluble (at room temperature) in the common organic solvents ($\text{CH}_3)_2\text{CO}$, $\text{C}_2\text{H}_5\text{OH}$, CH_3OH , CH_3CN , CH_3NO_2 , and $(\text{CH}_3)_2\text{SO}$. A green-yellow solution was obtained after several days only when the product was kept in $(\text{CH}_3)_2\text{SO}$ under prolonged stirring and slight heating. For all the reactions carried out the product yield (assuming the formulation $\text{Cu(II)(6-mp}^{2-}) \cdot \text{H}_2\text{O}$; see Analytical Results) was almost 100%.

Cu(II)–heterocycle competitive reactions. These were carried out systematically modifying the sequence of the metal–heterocycle reactions at different pH values, as is schematically shown below:



where M is Cu(II), L_1 is allopurinol, L_2 is hypoxanthine, L_3 is 6-mercaptapurine, X is metallic salt counterion, $[M + L_i]$ is chemical equilibrium between these reagents and the coordination compound formed, and $(L_i + L_{ii} + \dots)$ is solvated ligands.

In a typical reaction, 1 mmol of allopurinol was added to 100 ml of the specific buffer solution and the mixture was treated as under “Cu(II)–6-mercaptapurine reactions.” One millimole of the respective metallic salt was added to this solution, shortly forming (for pH values from 4 to 13) a blue suspension (the final product was reported before (7)) which was maintained under stirring and boiling for several hours; no changes were observed. One millimole of 6-mercaptapurine was added to this suspension at the same conditions; the mixture color changed from blue to green with time.

Finally, after several days, the reaction mixture was the same as that obtained in all the cases under "Cu(II)–6-mercaptapurine reactions," and the solid was treated in the same way. The product obtained (8) from the respective Cu(II)–allopurinol typical reaction at pH 1 (except for $X = \text{CH}_3\text{CO}_2^-$) was kept in solution at boiling conditions. The 6-mercaptapurine added to this solution formed the same green suspension, and the solid obtained was treated as before. The Cu(II)–allopurinol reaction yield also the same blue suspension from this typical reaction at pH 1 ($X = \text{CH}_3\text{CO}_2^-$). The following reaction step was carried out as before, and the same dark green product was also obtained.

The product was also the same (i.e., the dark green powder) from the systematically modified competitive reactions of the heterocyclic ligands (allopurinol and 6-mercaptapurine, hypoxanthine, and 6-mercaptapurine or even more, allopurinol, hypoxanthine, and 6-mercaptapurine) toward Cu(II) at several pH values and by employing diverse metallic salt counterions.

Methanolic Medium

For each one of the reactions carried out in this medium, the metallic salt counterion (from $X = \text{NO}_3^-$ to CH_3CO_2^-) was systematically modified as under Aqueous Medium.

Cu(II)–6-mercaptapurine reactions. One millimole of 6-mercaptapurine was dissolved (upon stirring, boiling, and refluxing at atmospheric pressure) in 100 ml of CH_3OH . One millimole of the respective metallic salt (previously dissolved in ca. 10 ml of CH_3OH) was added to the pale yellow solution. A green suspension was obtained and maintained under these conditions for several days; no further changes were observed. The solid formed (dark green) was isolated, purified, and dried as stated before.

Cu(II)–heterocycle competitive reactions. These reactions were carried out under the same scheme as in the aqueous medium. In a typical reaction, 1 mmol of 6-oxopurine was dissolved in 100 ml of CH_3OH under stirring, boiling, and refluxing at atmospheric pressure. The respective metallic salt was added to the colorless solution. A blue suspension was obtained which was maintained under the same conditions for several days, with no additional changes observed. Then, 1 mmol of 6-mercaptapurine was added to this suspension, turning to green with time. It was maintained under the experimental conditions stated before for several days; no changes were detected. The product (dark green) was isolated, purified, and dried as previously mentioned.

All the competitive Cu(II)–heterocycle methanolic reactions carried out yield also the same dark green product. The purity of the Cu(II) compound here studied was confirmed by analyzing the X-ray powder diffraction pattern of

all the solid products obtained from the competitive reactions and comparing it with the correspondent ones of both the free heterocyclic ligands and the Cu(II) compounds with the respective organic ligands allopurinol and hypoxanthine obtained under the same reaction conditions.

PHYSICAL MEASUREMENTS

Infrared (IR) spectra of all the samples were obtained as nujol mulls (CsI plates) in the $4000\text{--}200\text{ cm}^{-1}$ range by employing a 598 Perkin Elmer spectrometer. Electronic spectra (350–1100 nm) of the powdered samples were measured by the specular reflectance method in a 160-A Shimadzu equipment, and by using BaSO_4 as reference. Electronic spectra (200–1100 nm) of $(\text{CH}_3)_2\text{SO}$ solutions of the solvated compound were also obtained with the same equipment. Thermogravimetric measurements were carried out in a DT-30 Shimadzu equipment by using $\text{N}_2(\text{g})$ as carrier gas and $5^\circ\text{C}/\text{min}$ as heating rate. The magnetic susceptibility at room temperature was measured by the modified Gouy method using a Johnson Matthey balance and employing $\text{Hg}[\text{Co}(\text{SCN})_4]$ as calibration agent. The variable field and temperature magnetic susceptibility measurements were carried out by using a SQUID Quantum Design magnetometer from 2 to 300 K and from 10^3 to 5×10^4 G. The magnetic measurements for each magnetic field were performed both increasing and decreasing the temperature. They were corrected considering both the cell and the sample diamagnetic contributions. EPR spectra (X -band) of the powdered samples were obtained in a 200-D Bruker spectrometer at room and liquid nitrogen temperatures. An EPR spectrum (X -band) of the $(\text{CH}_3)_2\text{SO}$ frozen solution of the solvated compound was obtained only at liquid nitrogen temperature. The g values obtained were standardized against the absorption of diphenylpicrylhydrazyl (DPPH) at 2.0043. X-ray powder diffraction patterns of the organic ligands 6-oxopurine, allopurinol, and 6-mercaptapurine and several samples of the Cu(II) coordination compound obtained were taken in XD-5A Shimadzu and D-500 Siemens diffractometers. Microanalysis determination (C, H, N) was performed by the Chemistry Department at the University College of London and confirmed employing a 240-C Perkin Elmer equipment.

The samples obtained were previously exposed to atmosphere for several days before performing the analytical and the thermal studies. All the other physical measurements were carried out with the freshly obtained dried samples.

RESULTS AND DISCUSSION

The Cu(II) coordination compound obtained was the same irrespective of the pH values explored, the metallic salt counterion used, the metal:ligand molar ratios employed, and the sequence in the competitive Cu(II)–heterocycle

reactions performed. The same product was obtained by modifying the reaction medium, CH_3OH in this case. This compound appears to be of both remarkable kinetic and thermodynamic stabilities. To our knowledge, there is no example among the purine-type heterocycles with such reactivity and with the specific and selective coordination mode toward Cu(II) as that shown by 6-mp^{2-} in this study.

Analytical Results

All the samples analyzed are in agreement with the formulation $\text{Cu(II)}(6\text{-mp}^{2-})\cdot\text{H}_2\text{O}$. Found: 25.55% (C), 1.52% (H), 23.84% (N); expected for $\text{Cu}(\text{C}_5\text{H}_2\text{N}_4\text{S}^{2-})\cdot\text{H}_2\text{O}$: 25.91% (C), 1.73% (H), 24.17% (N).

Infrared (IR) Results

Figures 2 and 3 show, respectively, the medium and low-energy IR spectra of the free heterocyclic ligand and $\text{Cu(II)}(6\text{-mp}^{2-})$. Table 1 shows the assignments made to the spectral bands of the free heterocyclic ligand (9–16).

The IR spectrum of the free ligand 6-mercaptopurine shows a band at 3425 cm^{-1} ($\nu_{\text{N-H}}$), which does not exist in

the IR spectrum of the coordination compound. This is in agreement with the N–H deprotonation of the organic ligand in the Cu(II) compound. The bands in the IR spectrum of 6-mercaptopurine associated with $\nu_{\text{C-H}}$ vibrational modes (3140 and 3090 cm^{-1}) are not clearly shown in the IR spectrum of the Cu(II) compound and indicate a strong electronic modification of the nearest sites to the C–H groups. The band at 1610 cm^{-1} ($\delta_{\text{N-H}}/\nu_{\text{C=C}}/\nu_{\text{C=N}}$) in the free ligand IR shows a shift to lower energy (1580 cm^{-1}) in the Cu(II) compound IR, in agreement with the deprotonation stated before and the endocyclic coordination of the heterocycle.

The band appearing at 1520 cm^{-1} ($\nu_{\text{C=N}}/\text{ring vib.}$) in the free ligand IR spectrum is not observed in the IR spectrum of the Cu(II) compound. The 6-mercaptopurine IR band (1410 cm^{-1}) associated with several endocyclic groups vibrational modes ($\nu_{\text{C-N}}/\nu_{\text{C-C}}/\text{ring vib.}$) is also not present. This same spectral behavior is shown for the band at 1275 cm^{-1} ($\nu_{\text{C-N}}/\text{ring vib.}$) in the free ligand IR. Again, these spectral modifications are in agreement with the coordination of 6-mercaptopurine in a deprotonated state through endocyclic sites. The IR spectrum of 6-mercaptopurine shows a band at 1150 cm^{-1} ($\nu_{\text{C=S}}/\text{ring vib.}$) which is absent

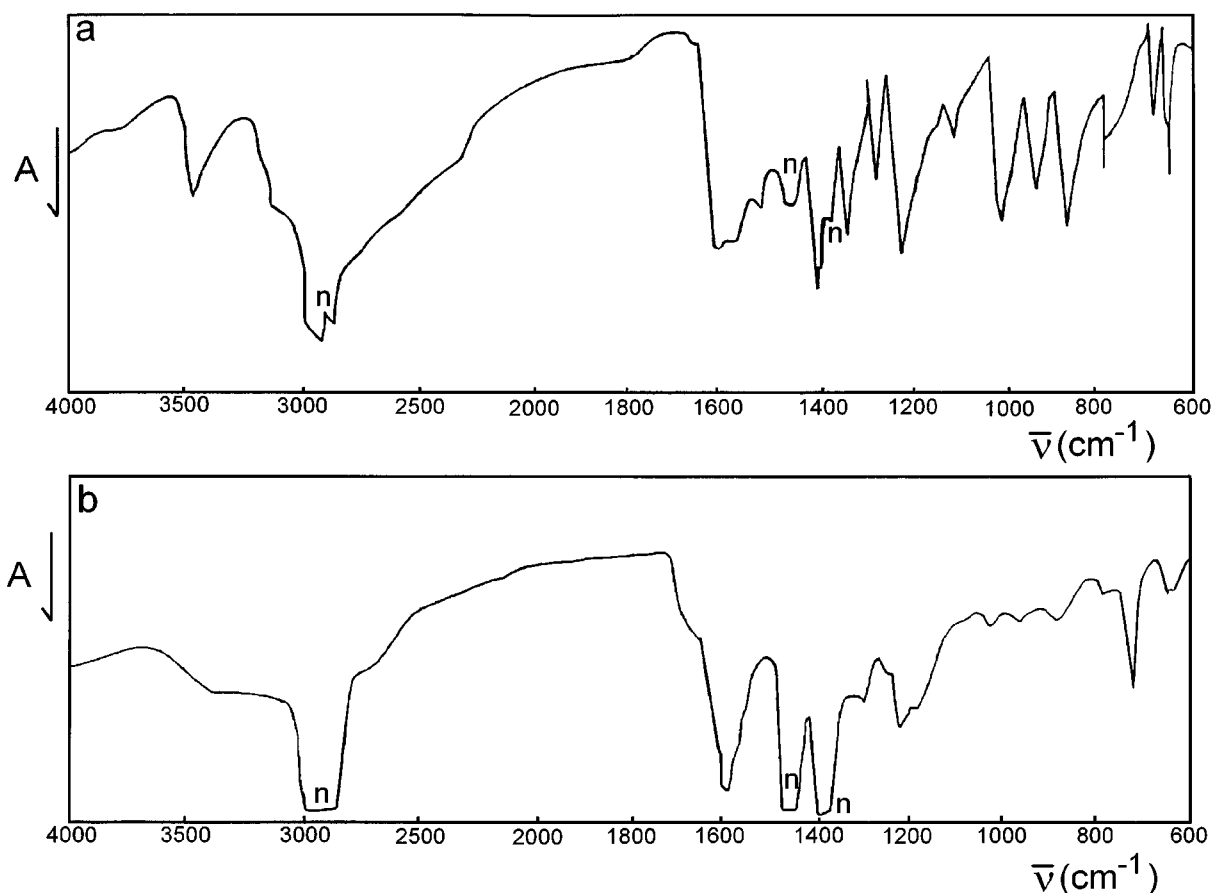


FIG. 2. IR spectra ($4000\text{--}600\text{ cm}^{-1}$) of (a) 6-mercaptopurine and (b) $[\text{Cu(II)}(6\text{-mp}^{2-})]_n$. n, nujol bands.

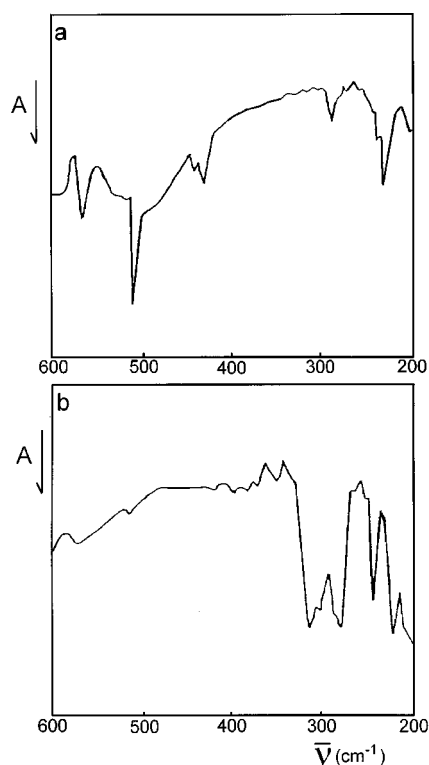


FIG. 3. IR spectra (600–200 cm^{-1}) of (a) 6-mercaptopurine and (b) $[\text{Cu}(\text{II})(6\text{-mp}^{2-})]_n$.

in the Cu(II) compound IR spectrum and suggests the participation of the exocyclic S(6) atom (together with endocyclic groups) in the metallic bonding. Related to this last proposition, the bands that appear at 1575, 1345 and

TABLE 1
IR Bands Assignments of the Free Heterocycle
6-Mercaptopurine

$\bar{\nu}$ (cm^{-1})	Assignments
3425	$\nu_{\text{N-H}}$ arom.
3140	$\nu_{\text{C-H}}$ arom.
3090	$\nu_{\text{C-H}}$ arom.
1610	$\delta_{\text{N-H}}/\nu_{\text{C=C}}/\nu_{\text{C=N}}$
1575	$\nu_{\text{R-N-C=S}}$ (I)
1520	$\nu_{\text{C=N}}$ /ring vib.
1410	$\nu_{\text{C-N}}/\nu_{\text{C-C}}$ /ring vib.
1345	$\nu_{\text{R-N-C=S}}$ (II)
1275	$\nu_{\text{C-N}}$ /ring vib.
1220	$\delta_{\text{CNC}}/\delta_{\text{NCN}}$ /ring vib.
1150	$\nu_{\text{C=S}}$ /ring vib.
1115	$\nu_{\text{R-N-C=S}}$ (III)
1010	$\delta_{\text{C-H}}/\delta_{\text{C-N}}$ /ring vib.
930	$\delta_{\text{C-H}}$ /imidazolic ring vib.
870	$\delta_{\text{C-H}}$ /ring vib.
780	$\delta_{\text{C-H}}$ /ring vib.
650	$\nu_{\text{C-S}}$ /ring vib.
600	Ring vib.
570–210	Nonassigned

Note. ν , stretching vibrational mode; δ , bending vibrational mode

1115 cm^{-1} ($\nu_{\text{R-N-C=S}}$) in the 6-mercaptopurine IR spectrum show a noticeable perturbation in the Cu(II) compound IR spectrum, together with the absence of some of them. This spectral pattern is also strongly suggestive of the S(6) atom participation in the metallic bonding of the heterocyclic ligand in the Cu(II) coordination compound. On the other hand, the IR spectrum of the coordination compound in the 1100–600 cm^{-1} range shows remarkable modifications (in frequency and intensity) of bands associated with vibrational modes of both the endocyclic groups (e.g., the C–H groups) and the exocyclic groups (i.e., the C–S group), in agreement with the involvement of the S(6) and N atoms in the metallic bonding of 6-mp^{2-} .

Finally, bands at 317, 275, 240, and 216 cm^{-1} appear in the low-energy IR spectrum of the Cu(II) coordination compound. These bands might be related to the $\nu_{\text{Cu-S}}$ and $\nu_{\text{Cu-N}}$ vibrational modes.

Electronic Spectroscopy Results

The electronic spectrum (350–1100 nm) of powdered Cu(II)(6- mp^{2-}) shows (Fig. 4a) a complex structure. In the blue region a broad and asymmetric band appears ($\lambda_{\text{max}} = 411 \text{ nm}$). From the low-energy side of this band, an absorption step by step decrease is observed, until the near-infrared limit is reached. The spectral features could be associated both with a metal–ligand charge transfer process and with the Cu(II) $d-d$ electronic transitions. Although the above spectral characteristics difficult a clear dilucidation of

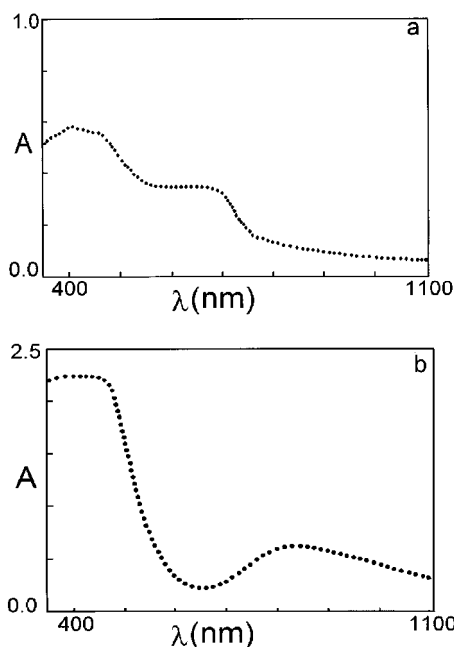


FIG. 4. Electronic spectra (350–1100 nm) of (a) powdered $[\text{Cu}(\text{II})(6\text{-mp}^{2-})]_n$ and (b) $(\text{CH}_3)_2\text{SO}$ solution of $[\text{Cu}(\text{II})(6\text{-mp}^{2-})]_n$.

the Cu(II) geometry, they let us suspect the existence of a distorted tetracoordinated environment around the metallic center.

The electronic spectrum (350–1100 nm) of the Cu(II) coordination compound solvated in $(\text{CH}_3)_2\text{SO}$ (Fig. 4b) shows a broad and asymmetric band at ca. 406 nm, which is assigned as above. The broad and asymmetric band associated with Cu(II) $d-d$ transitions appears at ca. 834 nm. This last spectral behavior might be attributed to changes in the Cu(II) coordination sphere, perhaps due to the presence of solvent molecules in it, to dissociative processes in the Cu(II) compound, or to both.

Thermogravimetric Results

The atmosphere exposed powdered sample shows a mass loss attributed to the process $\text{Cu(II)(6-mp}^{2-}) \cdot \text{H}_2\text{O} \rightarrow \text{Cu(II)(6-mp}^{2-})$. The temperature range (ca. 90–100°C) in which this loss occurs is also in agreement with the suggestion that the H_2O molecule is not involved in the Cu(II) coordination sphere, as was also inferred from the absence of the $\nu_{\text{M-OH}_2}$ vibrational mode in the low-energy IR spectrum of the dried Cu(II) compound. Finally, the thermal decomposition of the anhydrous Cu(II) system starts at ca. 320°C and it is attributed to the thermal heterocyclic ligand modification.

EPR Spectral Results

The X-band ($\nu = 9.244$ GHz) EPR spectra (Fig. 5a) of all the powdered samples of the Cu(II) coordination compound, both at room and at liquid nitrogen temperatures, are the same.

This spectral behavior could be associated with the presence of a nearly static structure around Cu(II) in this temperature range. The shape of the line in the high-field region let us suspect the existence of Cu(II)–Cu(II) magnetic interactions. The existence of an anisotropic g tensor can be inferred, with the components $g_1 = 2.02$, $g_2 = 2.09$, and $g_3 = 2.20$. From these, the parameter $R = (g_2 - g_1)/(g_3 - g_2) = 0.576$ let us propose a noticeable tetragonality around Cu(II). On the left side of the main absorption band a shoulder is observed ($g = 2.44$). The relative intensities of this shoulder and of the one associated with $g = 2.20$ makes it difficult to relate the absorption with $g = 2.44$ to the g_{\parallel} component. In fact, when analyzing the asymmetry of the main absorption, an overlapping of g_{\perp} and g_{\parallel} can be suggested. At this level of the study, it is difficult to discern about the detailed nature of such absorption, although it is possible to consider here hyperfine structure features.

The X-band ($\nu = 9.204$ GHz) EPR spectrum of $(\text{CH}_3)_2\text{SO}$ frozen solution (77 K) of the solvated Cu(II) coordination

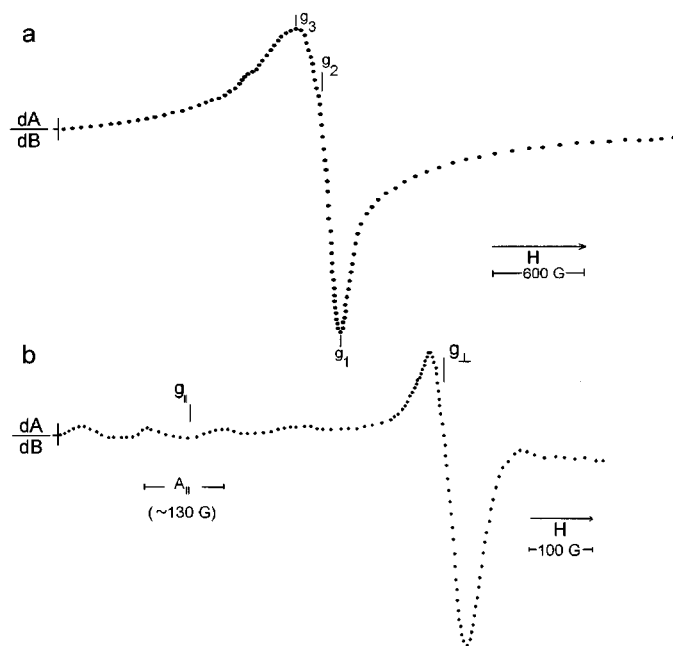


FIG. 5. X-band EPR spectra of $[\text{Cu(II)(6-mp}^{2-})]_n$ (a) in powdered solid state at 300 K ($\nu = 9.244$ GHz) and (b) in $(\text{CH}_3)_2\text{SO}$ frozen solution (77 K) ($\nu = 9.204$ GHz).

compound is shown in Fig. 5b. The spectral pattern (axial-type) is very different from that in the solid state. For the case in discussion, an anisotropic g tensor, with values of $g_{\perp} = 2.08$ and $g_{\parallel} = 2.40$, is also inferred. The spectrum in the high-field region also indicates the existence of metal–metal magnetic coupling. In the low-field region, the four absorptions are attributed to a hyperfine structure; the A_{\parallel} value (ca. 130 G) is associated with a significant e^- -nuclei coupling. It is necessary to point out that the EPR spectral pattern resembles the one shown by some Cu(II) compounds in solution that show a pentacoordinated environment (square pyramidal) in the solid state (17). It is possible to propose that the ground electronic state of the Cu(II) centers lies mainly upon the $d_{x^2-y^2}$ orbitals.

X-Ray Powder Diffraction Patterns Results

The X-ray diffraction pattern ($10-70^\circ 2\theta$) of the free organic ligand shows several signals, mainly in the low- 2θ region. However, the respective diffraction pattern ($10-60^\circ 2\theta$) of several powdered samples of the Cu(II) coordination compound indicates an amorphous character. This could be associated both with the synthesis conditions and with the complex polynuclear character of the Cu(II) compound. Slow evaporations of both aqueous and methanolic filtrates of the original reaction mixtures yield scarce mass of the same amorphous system.

In summary, with all the experimental results previously discussed, the existence of a Cu(II) coordination compound that only shows heterocyclic donor atoms of the deprotonated 6-mp²⁻ ligand in the metallic coordination sphere can be considered. The spectroscopic data would be in concordance with the metallic bonding of the exocyclic S(6) atom and endocyclic N atoms forming a distorted tetracoordinated Cu(II) environment. With respect to the nature of these last atoms, the electron donor properties of those corresponding to the imidazolic ring would make them the most favorable ones, because of the high basicity of the N(9) atom, and of the adequate structural disposition of the N(7) atom in constructing (together with the S(6) atom) bidentate bonding toward metallic centers. This metallic bonding mode is characterized by a noticeable metal–ligand thermodynamic stability.

In order to obtain a possible structural arrangement for this Cu(II) compound, in agreement with all the results previously discussed and with the existence of a polynuclear character, systematically modified molecular models were made. From these, only one arrangement, shown in Fig. 6, is self-consistent.

In this, the Cu(II) atoms are simultaneously bridged by the S(6) and the N(7)/N(9) atoms of the bideprotonated ligand. The structural arrangement would not be planar, with the Cu(II) atoms in a roughly distorted tetracoordinated environment (i.e., flattened tetrahedral geometry). This structural proposition for the novel Cu(II) coordination compound would implicate the existence of an unexplored metallic bonding mode for the heterocyclic ligand, also in a nonfrequent deprotonation level. This roughly bidimensional network is not frequent in the metal coordination chemistry. Very scarce examples of this class have been reported to date, one of them being the system [Cu(II)(imidazolate⁻)₂]_n (18–20), in which the mono-

anionic ligands are bridging the Cu(II) atoms in two directions. Two other examples of this type are the compounds [Cu(II)(methylpyrazolate⁻)₂]_n and [Cu(II)(chloropyrazolate⁻)₂]_n, in which the Cu(II) atoms are linked through the N atoms of the pyrazolate⁻ rings (21). In these structures the Cu(II) environments are, respectively, flattened tetrahedrals (21) or alternating planar tetracoordinated and flattened tetrahedrals (18–20). Also, in all these few examples the 1:2 metal:heterocycle stoichiometry is present. The Cu(II) compound in discussion here is the first example of a 1:1 Cu(II):6-mp²⁻ system for which a spectroscopic and magnetic characterization (see below) has been made.

Only one example of the M(II)(6-mp²⁻) type has been reported up to date (14), which corresponds to the formulation Cd(II)(6-mp²⁻)·H₂O. Unfortunately, only a limited study was made without advances in its structural arrangement and in the detailed metallic bonding of the heterocyclic ligand.

Magnetic Studies Results

The magnetic study of the Cu(II) compound under discussion was made in the 2–300 K range and external magnetic fields of 10³, 10⁴, 3 × 10⁴, and 5 × 10⁴ G. When plotting the $\bar{\chi}$ (emu/Cu(II)) values versus T (K) for the respective magnetic fields, a small decrease of the magnetic susceptibility with the increase of the magnetic field intensity was observed. The general pattern of the curves is in agreement with a Curie–Weiss behavior; the fitting process of the Curie–Weiss equation ($\chi = \chi_0 + C/(T - \theta)$) to the experimental data was very good, and the θ (<0) values obtained for all the magnetic fields indicate the existence of an antiferromagnetic coupling in the solid product. This type of magnetic coupling is confirmed plotting $\bar{\chi}T$ versus T for all the magnetic field intensities. In this representation (Fig. 7) a continuous decrease of $\bar{\chi}T$ values with descending

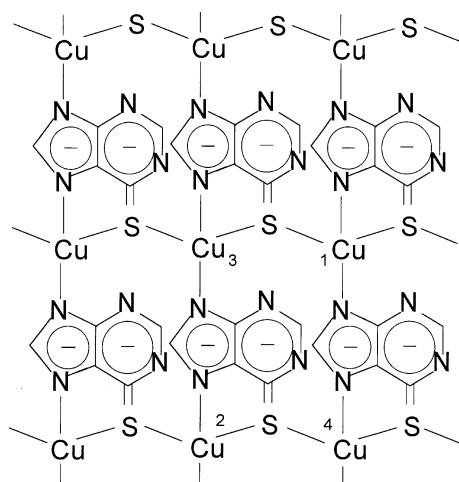


FIG. 6. Schematic drawing of the structural arrangement proposition for [Cu(II)(6-mp²⁻)]_n.

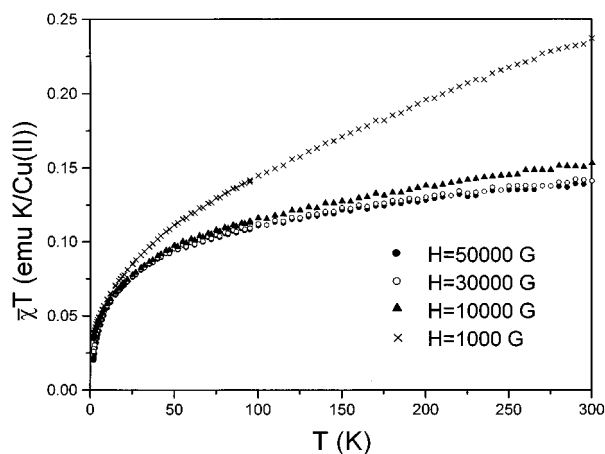


FIG. 7. $\bar{\chi}T$ (emu K/Cu(II)) – T (K) data for [Cu(II)(6-mp²⁻)]_n at several magnetic fields.

T is observed, and at temperatures lower than 100 K, the slope increases continuously as $T \rightarrow 0$ K. This pattern indicates an antiferromagnetic coupling in the sample analyzed.

We selected the linear chain model of coupled $S = 1/2$ spins to analyze the magnetic features of the structural proposition mentioned before. The magnetic susceptibility is described by the Bonner–Fisher equation

$$\bar{\chi}_{\text{BF}} = \frac{N\beta^2 g^2}{kT} \left[\frac{0.025 + 0.14995x + 0.30094x^2}{1 + 1.9862x + 0.68854x^2 + 6.0626x^3} + \bar{\chi}_0 \right] \times (1 - \rho) + \frac{N\beta^2 g^2}{2kT} \rho, \quad [1]$$

where $x = |J|/kT$, and the other symbols have their usual meaning. With this equation, very good fitting results were obtained for the whole temperature and magnetic field ranges. The value of the spectroscopic g tensor (2.09) was maintained constant in this process. The parameters obtained were $H = 1000$ G: $J = -7.59 \pm 0.15 \text{ cm}^{-1}$, $\rho = 0.1748 \pm 0.0015$, $\bar{\chi}_0 = 1.549 \times 10^{-3} \pm 1.33 \times 10^{-4} \text{ emu/tetranuclear unit}$; $H = 10,000$ G: $J = -6.67 \pm 0.17 \text{ cm}^{-1}$, $\rho = 0.1608 \pm 0.0014$, $\bar{\chi}_0 = 8.09 \times 10^{-5} \text{ emu/tetranuclear unit}$; $H = 30,000$ G: $J = -4.64 \pm 0.16 \text{ cm}^{-1}$, $\rho = 0.1090 \pm 0.003$, $\bar{\chi}_0 = 8.09 \times 10^{-5} \text{ emu/tetranuclear unit}$; $H = 50,000$ G: $J = -4.13 \pm 0.13 \text{ cm}^{-1}$, $\rho = 0.0720 \pm 0.003$, $\bar{\chi}_0 = 8.09 \times 10^{-5} \text{ emu/tetranuclear unit}$. The J values indicate a very weak intensity for the intrachain antiferromagnetic coupling. The ρ values (assumed as the mole fraction of noncoupled $S = 1/2$ spins) are consistent with the Curie–Weiss behavior in the low-temperature region.

The presence of the noncoupled $S = 1/2$ spins makes it difficult to observe the $\bar{\chi}$ maxima as a function of temperature in the four different magnetic fields curves. The maxima are predicted by Eq. [1] with $\rho = 0$ (by employing the other fitting parameters obtained before) to be localized in the 7–13 K range for the four magnetic fields. This is in concordance with the typical $\bar{\chi} - T$ behavior for a system with a very weak antiferromagnetic coupling.

The structural proposition for the Cu(II) compound also considers the possibility of interchain magnetic interactions, in addition to the intrachain ones. To analyze this possibility, a molecular field approximation was included, for which the magnetic susceptibility is calculated as

$$\bar{\chi} = \frac{\bar{\chi}_{\text{BF}}}{1 - (2zJ'\bar{\chi}_{\text{BF}}/N\beta^2 g^2)}, \quad [2]$$

where $\bar{\chi}_{\text{BF}}$ is the magnetic susceptibility for a linear chain of coupled $S = 1/2$ spins described by Eq. [1], z is the number of nearest neighboring chains and J' is the interchain mean-field magnetic coupling parameter. The fitting process for this expression was very good, and the magnetic parameters obtained were (for $g = 2.09$ and $z = 4$): $H = 1000$ G:

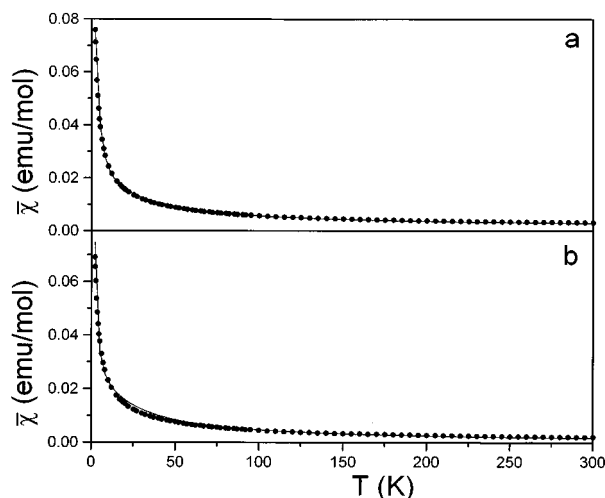


FIG. 8. $\bar{\chi}$ (emu/tetranuclear unit) as a function of T (K) for $[\text{Cu(II)(6-mp}^2\text{-)}]_n$ (a) from the linear chain magnetic model with a mean-field approximation ($H = 1000$ G) and (b) from the C_{2v} tetranuclear cluster magnetic model ($H = 10,000$ G). Dotted lines are experimental data; solid curves are theoretical values.

$J = -11.34 \pm 0.27 \text{ cm}^{-1}$, $J' = -0.45 \pm 0.06 \text{ cm}^{-1}$, $\rho = 0.21 \pm 0.001$, $\bar{\chi}_0 = 1.09 \times 10^{-3} \pm 3.7 \times 10^{-5} \text{ emu/tetranuclear unit}$; $H = 10,000$ G: $J = -11.58 \pm 0.19 \text{ cm}^{-1}$, $J' = -0.67 \pm 0.05 \text{ cm}^{-1}$, $\rho = 0.21 \pm 0.001$, $\bar{\chi}_0 = 1.90 \times 10^{-4} \pm 2.6 \times 10^{-5} \text{ emu/tetranuclear unit}$; $H = 30,000$ G: $J = -11.58 \pm 0.31 \text{ cm}^{-1}$, $J' = -1.56 \pm 0.01 \text{ cm}^{-1}$, $\rho = 0.22 \pm 0.002$, $\bar{\chi}_0 = 7.59 \times 10^{-5} \pm 3.8 \times 10^{-5} \text{ emu/tetranuclear unit}$; $H = 50,000$ G: $J = -11.20 \pm 0.34 \text{ cm}^{-1}$, $J' = -2.54 \pm 0.17 \text{ cm}^{-1}$, $\rho = 0.21 \pm 0.002$, $\bar{\chi}_0 = 5.65 \times 10^{-5} \pm 4.1 \times 10^{-5} \text{ emu/tetranuclear unit}$. The corresponding theoretical values from Eq. [2] are shown in Fig. 8a together with the experimental data for $H = 1000$ G.

The results support the existence of very weak both intra- and interchain antiferromagnetic coupling throughout the network proposed for the polynuclear Cu(II) coordination compound. In a further step of the magnetic study, the tetranuclear cluster magnetic model of coupled $S = 1/2$ spins in the T_d, D_{2d}, D_2 , and C_{2v} symmetries was employed to fit the experimental data. The best results were obtained for the C_{2v} symmetry. In this approximation (22), $J_1 \neq J_2 \neq J_3 = J_4$. J_1 and J_2 would represent the superexchange magnetic coupling parameters for the two diagonal pairs (1–2; 3–4) of $S = 1/2$ spins in a tetranuclear unit of the network shown in Fig. 6 (see numbering there); J_3 and J_4 would represent the corresponding magnetic parameters for the pairs (1–3 or 2–4; 1–4 or 2–3) of nondiagonal $S = 1/2$ spins. From the fitting process, the following parameters were obtained (for fixed $g = 2.09$): $H = 1000$ G: $J_1 = -3.22 \pm 1.4 \text{ cm}^{-1}$, $J_2 = -10.12 \pm 0.96 \text{ cm}^{-1}$, $J_3 = J_4 = -3.26 \pm 0.47 \text{ cm}^{-1}$, $\bar{\chi}_0 = 0.00315 \text{ emu/tetranuclear unit}$, $\rho = 0.97 \pm 0.00097$; $H = 10,000$ G: $J_1 = -2.74$

$\pm 0.46 \text{ cm}^{-1}$, $J_2 = -9.27 \pm 0.68 \text{ cm}^{-1}$, $J_3 = J_4 = -3.12 \pm 0.20 \text{ cm}^{-1}$, $\bar{\chi}_0 = 0.002 \text{ emu/tetranuclear unit}$, $\rho = 0.97 \pm 0.00073$; $H = 50,000 \text{ G}$: $J_1 = -2.15 \pm 1.56 \text{ cm}^{-1}$, $J_2 = -7.96 \pm 0.55 \text{ cm}^{-1}$, $J_3 = J_4 = -2.16 \pm 0.52 \text{ cm}^{-1}$, $\bar{\chi}_0 = 0.0018 \text{ emu/tetranuclear unit}$, $\rho = 0.98 \pm 0.00064$.

From these results, an antiferromagnetic coupling between the unpaired electrons of the Cu(II) atoms involved in the constructing tetranuclear unit of the network previously proposed before can be suggested. The theoretical values from the corresponding equation (22) are shown in Fig. 8b together with the experimental data for $H = 10,000 \text{ G}$. From this approximation, one finds that $J_1 + J_3 + J_4$ is slightly lower than J_2 , in agreement with the low symmetry considered for the distorted bidimensional metallic network suggested for this Cu(II) compound. From the theoretical model, the possible existence of a relatively more favorable magnetic coupling pathway between the four types considered can be suggested. In this magnetic analysis, the ρ values are noticeable overestimated in the fitting process.

The two magnetic models explored can be considered qualitatively equivalent in the magnetic data description. In fact, both models let us propose the existence of magnetic coupling through tetranuclear Cu(II) units (the first one through interacting Cu(II) chains; the second one, as distorted tetranuclear Cu(II) units), and Cu(II)–Cu(II) antiferromagnetic coupling is inferred. In this coupling, the bridging electron donor groups appear to be the most favorable ones in constructing the superexchange magnetic coupling pathways. The very weak intensity in the antiferromagnetic coupling would appear to be related (in great measure) to distortions in the planes that contain the Cu(II) atoms (i.e., a distorted bidimensional network). However, at this level of experimental information and magnetic study, it is difficult to state the detailed structural correspondence for each one of the superexchange magnetic coupling parameters (J values). The presence of noncoupled $S = 1/2$ spins difficulties the magnetic characterization (e.g., the observation and study of the $\bar{\chi}$ maxima in the $\bar{\chi} - T$ curves). The noncoupled spins could be associated in part to the amorphous character of the solid product and the short-range order for the metallic network proposed.

Finally, the molar magnetization (\bar{M}) as a function of the magnetic field at constant temperature was analyzed using the Brillouin function. The good fitting to the experimental data at different constant temperatures let us estimate the respective total spin states S : 0.31 ($T = 2 \text{ K}$); 0.40 ($T = 5 \text{ K}$); 0.47 ($T = 10 \text{ K}$); 0.56 ($T = 20 \text{ K}$); 0.68 ($T = 50 \text{ K}$); 0.74 ($T = 100 \text{ K}$), and 0.80 ($T = 200 \text{ K}$). Figure 9 shows the case for $T = 10 \text{ K}$, for which negative magnetic fields were applied to the sample. The magnetization is fully reversible under these experimental magnetic conditions for the whole temperature range.

A gradual singlet ($S = 0$) state depopulation starting at 2 K and with the increase of temperature is deduced from

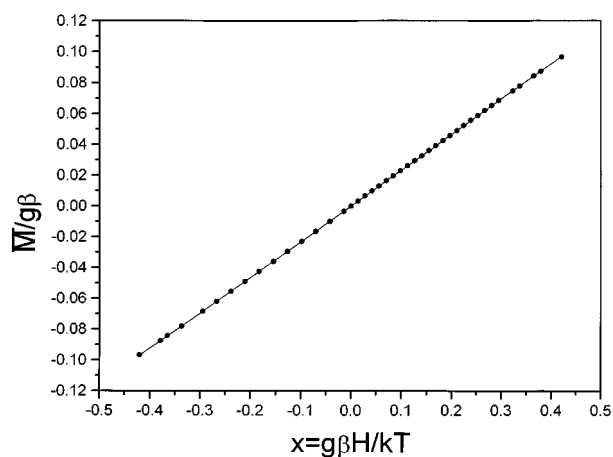


FIG. 9. $\bar{M}-H$ plot ($T = 10 \text{ K}$) of $[\text{Cu(II)(6-mp}^{2-})]_n$. Dotted line is experimental data; solid line is theoretical values from the Brillouin function.

the S values. Typical $\bar{M}-H$ magnetic patterns corresponding to an antiferromagnetic coupling (23) are also obtained in the $10\text{--}200 \text{ K}$ range.

CONCLUDING REMARKS

Several synthetic routes for the novel polynuclear compound $[\text{Cu(II)(6-mercaptapurinolate}^{2-})]_n$ were obtained. This system shows both a metal–ligand stoichiometry and a heterocyclic ligand deprotonation level, scarcely explored in the coordination chemistry of this organic molecule. The formation of the Cu(II) compound appears to be associated with noticeable kinetic and thermodynamic stabilities, also deduced from several Cu(II)–heterocyclic ligand competitive reactions. These stabilities could be associated with the high anionic character of 6-mp^{2-} and thus to its polycoordinating capability toward the metallic atoms, as is inferred from the spectroscopic data. These results support the involvement of the exocyclic S(6) atom and N atoms of the imidazolic moiety in the metallic bonding. The metal:ligand stoichiometry and polynuclear character of the Cu(II) compound allow us to suggest a 6-mercaptapurine coordination type not explored up to date. This is concerned with its polydirectional metallic bonding mode, which in turn favors the Cu(II)–Cu(II) magnetic coupling in a distorted tetra-coordinated geometry for Cu(II). The magnetic studies confirm the existence of magnetic coupling between the unpaired electrons of the Cu(II) atoms, this being of very weak antiferromagnetic character through both classes of superexchange magnetic coupling pathways postulated from the two magnetic models explored. The very weak magnetic coupling in the polynuclear Cu(II) compound studied here appears to be related both to the structural distortions through the metallic network and to the restricted

short-range order in this, in concordance with the amorphous character of the samples analyzed.

Finally, it is important to arise the high difficulty associated with the study of noncrystalline coordination compounds. In this context, the magnetic studies are an invaluable tool to advance in their characterization and to detect or to suggest certain phenomena at a molecular level.

ACKNOWLEDGMENTS

We thank Jorge Ramírez-Salcedo (IFC-UNAM), Max Azomoza-Palacios (UAM-Iztapalapa), Leticia Baños-López (IIM-UNAM), and Francisco Morales-Leal (IIM-UNAM) for the EPR spectra, thermal results, X-ray diffraction patterns, and magnetic susceptibility measurements, respectively. We also acknowledge CONACyT (Grant 3170-E) for partial financial support.

REFERENCES

1. A. G. Beaman and R. K. Robins, *J. Am. Chem. Soc.* **83**, 4038 (1961).
2. G. M. Brown, *Acta Crystallogr.* **B25**, 1338 (1969).
3. J. A. Nelson, J. W. Carpenter, L. M. Rose, and D. J. Adamson, *Cancer Res.* **35**, 2872 (1975).
4. "Nuclei Acid-Metal Ion Interactions" (T. G. Spiro, Ed.), Vol. 1. Wiley, New York, 1980.
5. J. R. Lusty, "Handbook of Nucleobase Complexes," Vol. I. CRC Press, Boca Raton, FL, 1990, and references therein.
6. E. Dubler and E. Gyr, *Inorg. Chem.* **27**, 1466 (1988).
7. R. Acevedo-Chávez, M. E. Costas, and R. Escudero, *J. Solid State Chem.* **113**, 21 (1994).
8. R. Acevedo-Chávez, M. E. Costas, and R. Escudero, *Inorg. Chem.* **35**, 7430 (1996).
9. N. Katsaros and A. Grigoratou, *J. Inorg. Biochem.* **25**, 131 (1985).
10. N. Kottmair and W. Beck, *Inorg. Chim. Acta* **34**, 137 (1979).
11. J. Brigando, D. Colaitis, and M. Morel, *Bull. Soc. Chim. Fr.* **10**, 3440 (1969).
12. P. Piperaki, N. Katsaros, and D. Katakis, *Inorg. Chim. Acta* **67**, 37 (1982).
13. R. Barbieri, E. Rivarola, F. Di Bianca, and F. Huber, *Inorg. Chim. Acta* **57**, 37 (1982).
14. L. Perelló, J. Borrás, L. Soto, F. J. Gordo, and J. C. Gordo, *Monats. Chem.* **115**, 1377 (1984).
15. N. Hadjiliadis and T. Theophanides, *Inorg. Chim. Acta* **15**, 167 (1975).
16. N. B. Behrens and D. M. L. Goodgame, *Inorg. Chim. Acta* **46**, 45 (1980).
17. N. Kitajima, K. Fujisawa, and Y. Moro-oka, *J. Am. Chem. Soc.* **112**, 3210 (1990).
18. J. A. J. Jarvis and A. F. Wells, *Acta Crystallogr.* **13**, 1027 (1960).
19. M. Inoue, M. Kishita, and M. Kubo, *Inorg. Chem.* **4**, 626 (1965).
20. H. C. Freeman, *Adv. Protein Chem.* **22**, 257 (1967).
21. A. M. V. Sadus, *Transition Met. Chem.* **20**, 46 (1995), and references therein.
22. J. W. Hall, W. E. Estes, E. D. Estes, R. P. Scaringe, and W. E. Hatfield, *Inorg. Chem.* **16**, 1572 (1977).
23. J. S. Miller, A. J. Epstein, and W. M. Reiff, *Chem. Rev.* **88**, 201 (1988).